Radial Compression to Transiently Achieve Higher Beta Poloidal in a Tokamak

Lu Qu and Ge Li

Abstract— **An increase in the magnetic strength of the vertical field will, in general, compress and heat plasmas, which thus allows high temperature, high density, and high beta to be reached. In this paper, according to the scaling laws for the magnetic compression, the scaling range of both the major-radius compression and the minor-radius compression is figured out. Then, the comparison between the major-radius compression and the minor-radius compression is carried out. It demonstrates that the minor-radius compression can obtain higher β_p of plasma. Consequently, we try to significantly enhance discharge parameters by the minor-radius compression by inserting the sets of the vertical-field coils in the experimental advanced superconducting tokamak (EAST) vacuum chamber. Afterward, the minor-radius compression based on EAST shot #34128 is deduced with $C_a = 1.5$ and $C_R = 0.925$, which increases β_p by 76.19%. It notes that the minor-radius compression is a promising way to effectively improve β_p in a tokamak. Finally, the preliminary design of the minor-radius compression, which includes the control system, the in-vessel vertical-field coils, and its fast-control power supply, is described.**

Index Terms— **Higher beta, magnetic compression, tokamak.**

I. Introduction

IN ORDER to improve the confinement and β for advanced tokamak, the control of the current density (or q profile) has been proposed as a method [1]. Gourdain *et al.* [2] used a straightforward definition of high β_p plasmas based on the toroidal current density alone. Therefore, high β_p can be realized by means of highly shift of the plasma magnetic axis under a possible route manifesting itself as equilibrium stability. Li [3], [4] suggests implementing such a route by magnetic compression in the experimental advanced superconducting tokamak (EAST).

In general, the magnetic compression can shape the plasma and maintain its radial current distribution, i.e., its safety factor q-profile [5], and thus allows high temperature and high density to be realized at the same time. Furthermore, control of the current density and the temperature can improve the confinement and β_p ($\beta_p \propto n_e T_e$) for an advanced tokamak. Therefore, it is a promising way to realize the high β_p to prepare efficient beam heating and decrease high turbulent transport [6] by magnetic compression.

The adiabatic compression of the plasma by a magnetic field in the Tuman tokamak device is described in [7]. The compression of the minor radius a, by a factor C, at constant R, was carried out by increasing the toroidal field B_t. The adiabatic toroidal compressors (ATCs) were designed to compress the plasma in major radius, by a factor of 2.3. The minor radius also shrunk, according to the law $a \propto R^{1/2}$ [5], [8], [9]. The parameters of the compressed plasma were measured, and the comparison with adiabatic compression was reported in [8]. The tangentially coinjected deuterium beam ions of the tokamak fusion test reactor project were accelerated from 82 to 150 keV during a major-radius compression experiment, accompanied by enhanced fusion neutron emission [10]. Unlike the ATC experiment, the plasma rotation was also observed, and its change during compression was roughly consistent with the conservation of angular momentum.

In this paper, the scaling range of the magnetic compression is figured out based on the scaling laws. Then, we compare the minor-radius compression with the major-radius compression. In consideration of the comparison result, the minor-radius compression is adopted to realize the higher parameters in the EAST, and a derivation is made based on the EAST shot #34128. Finally, the primary scheme of the minor-radius compression is given.

II. Scaling Laws for Magnetic Compression

Assuming perfect conductivity for the plasma, because the compression time is shorter than the diffusion time τ, the flux of the toroidal field B_t is conserved within the moving plasma, so two basic constraints are given as [5], [11]

$$a^2 B_t = \text{const} \tag{1}$$

$$\tau = 2\pi/q = \text{const} \tag{2}$$

where a is the minor radius and τ is the rotational transform angle. For collisional compression, we also have constraint on the plasma temperature T_e and density n_e

$$T_e n_e^{-2/3} = \text{const.} \tag{3}$$

In terms of the minor radius a and major radius R of the tokamak, the compression scaling laws are given as

$$n_e \to a^{-2} R^{-1} \tag{4}$$

$$T_e \to a^{-4/3} R^{-2/3} \tag{5}$$

$$B_t \to a^{-2} \tag{6}$$

$$B_p \to a^{-1} R^{-1} \tag{7}$$

$$I_p \to R^{-1} \tag{8}$$

$$\tau_e \to a R^{-1} \tag{9}$$

Manuscript received September 14, 2015; revised February 24, 2016; accepted March 7, 2016. Date of publication March 23, 2016; date of current version May 6, 2016. *(Corresponding author: Lu Qu.)*

The authors are with the Institute of Plasma Physics, Chinese Academy of Sciences, Hefei 230031, China (e-mail: qulu@ipp.ac.cn; lige@ipp.ac.cn).

Color versions of one or more of the figures in this paper are available online at http://ieeexplore.ieee.org.

Digital Object Identifier 10.1109/TPS.2016.2540649

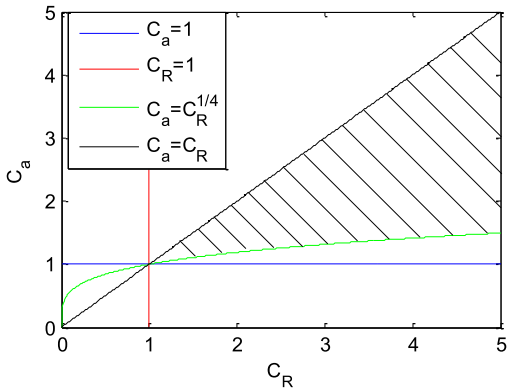

Fig. 1. Scaling range of the major-radius compression.

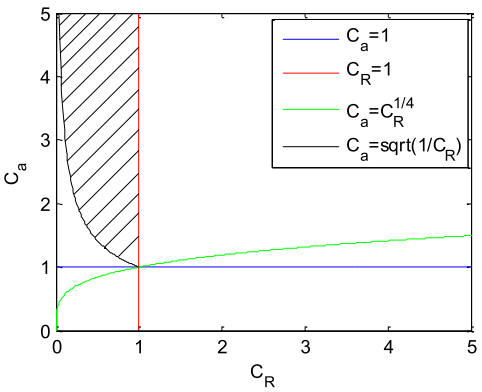

Fig. 2. Scaling range of the minor-radius compression.

$$\beta_t \rightarrow a^{2/3} R^{-5/3} \tag{10}$$

$$\beta_p \rightarrow a^{-4/3} R^{1/3} \tag{11}$$

where B_p is the magnetic flux of the poloidal field, I_p is the plasma current, and β_p is the poloidal beta.

III. Scaling Range for Magnetic Compression

An increase in the vertical field B_z can be used to compress R or a effectively. This technique provides a proven means for increasing the plasma density and temperature in tokamak beyond the level that can be achieved by resistive heating alone. For compressed plasma, define the minor and major radii as $a_{1,2}$ and $R_{1,2}$, respectively. The subscripts 1 and 2 refer to the initial and final states of compression. Thus, the scaling ratios are $C_a = (a_1/a_2)$ and $C_R = (R_1/R_2)$.

A. Major-Radius Compression

Major-radius compression compresses the plasma to its inboard boundary, so $C_a > 1$ and $C_R > 1$. If n_e, T_e, τ_e, and β_p are increased by the major-radius compression at the same time, then the scaling range is derived as

$$\begin{cases} C_a > 1 \\ C_R > 1 \\ C_R > C_a \\ C_a > \sqrt[4]{C_R}. \end{cases} \tag{12}$$

Therefore, the scaling range of the major-radius compression is shown in Fig. 1 (shadow zone).

B. Minor-Radius Compression

Minor-radius compression compresses the plasma to its outboard boundary, so $C_a > 1$ and $C_R < 1$.

As (9), $\boldsymbol{\tau_e}$ cannot be increased by the minor-radius compression. If $\boldsymbol{n_e}$, $\boldsymbol{T_e}$, and $\boldsymbol{\beta_p}$ are increased by the minor-radius compression, then the scaling range is derived as

$$\begin{cases} C_a > 1 \\ C_R < 1 \\ C_a > \sqrt{\dfrac{1}{C_R}}. \end{cases} \tag{13}$$

Therefore, the scaling range of the minor-radius compression is shown in Fig. 2 (shadow zone).

TABLE I
Comparison Between Major-Radius and Minor-Radius Compression in EAST

Plasma parameter	Before compression	minor-radius C_a=1.5, C_R=0.925	major-radius C_a=1.1, C_R=1.239
a (m)	0.461	0.3073	0.4191
R (m)	1.873	2.0249	1.5117
n_e ($\times 10^{19}$m^{-3})	1.8	3.7463	2.6985
T_e (kev)	1.6	2.6082	2.0958
I_p (MA)	1	0.925	1.239
B_t (T)	2.45	5.5125	2.9645
B_z (T)	0.1103	0.1503	0.1503
β_p	0.097	0.1709	0.1026
C_W	-	1.5475	1.5111

IV. Comparison Between Major-Radius and Minor-Radius Compression

The major-radius compression is beneficial to minimize the pulsed vertical magnetic field requirements and reach final low-aspect-ratio final state; while the minor-radius compression is recommended in favor of optimizing the energy balance in the initial ohmic-heating state, and minimizing the skin-effect problems and the plasma rotation [12].

In this section, the comparison between the major-radius and minor-radius compression is made based on the discharge parameters of EAST shot #34128 [13], [14], which is the representative discharge with the large plasma current of 1 MA. Assume that the fast-control vertical magnetic field with 0.04 T is applied to compress the plasma at 5.01 s, and the calculation results are shown in Table I.

The calculation results demonstrate that the minor-radius compression has higher discharge parameters than the major-radius compression under the same additional vertical field 0.04 T. The gain of the plasma energy $C_W = C_a^{4/3} C_R^{4/3}$ increases by 154.75%. It is also clear that n_e and T_e have an increase in 109.12% and 63.01%, respectively, by the minor-radius compression. In particular, it is obvious for β_p

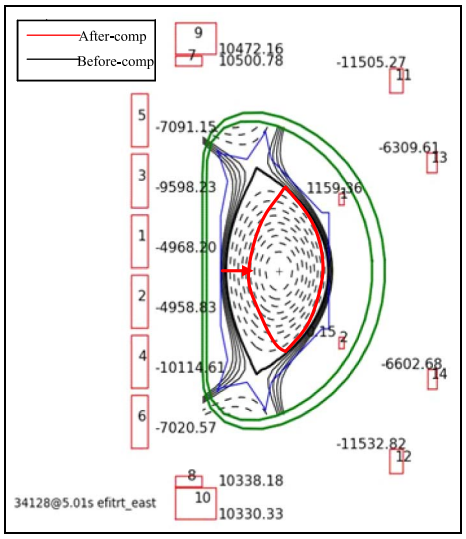

Fig. 3. Schematic of the minor-radius compression in EAST.

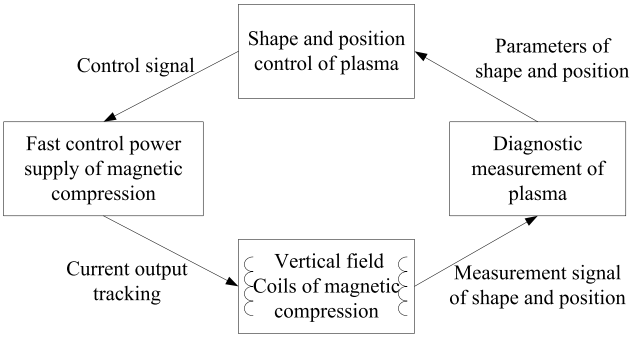

Fig. 4. Schematic of the control system of the radial magnetic compression.

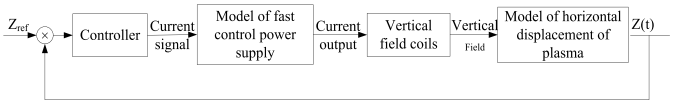

Fig. 5. Control diagram of the radial magnetic compression.

to increase by only 5.77% by the major-radius compression, while increasing by 76.19% by the minor-radius compression. Therefore, it is a promising way to effectively improve β_p by the minor-radius compression. It is obvious that the toroidal field B_t increases from 2.45 to 5.5125 T during the minor-radius compression.

EAST shot #34128 is taken as an example here to demonstrate the scaling of the plasma shape by the minor-radius compression with $C_a = 1.5$, $C_R = 0.925$, and the in-vessel vertical-field coils working at 5.01 s. The scaling schematic is shown in Fig. 3.

V. Solution of Minor-Radius Compression in EAST

Based on the comparison results, we try to enhance discharge parameter significantly, particularly β_p, by the minor-radius compression with inserting a set of vertical-field coils in the EAST vacuum chamber for shaping the plasma. In this section, the scheme of the minor-radius compression in EAST is described.

A. Control System of Radial Magnetic Compression

In order to rapidly compress the plasma in the radial direction and maintain the radial equilibrium of the plasma, the control system of the radial magnetic compression is required to control the radial displacement in time, which includes the fast-control power supply for the magnetic compression and the in-vessel vertical-field coils.

The working procedure of the control system of the radial magnetic compression is shown in Fig. 4. First, the plasma control system detects the radial displacement of the plasma and calculates the corresponding excitation current of the vertical-field coils for magnetic compression. Then, the required current signal is sent to the fast-control power supply. The fast-control power supply tracks the input signal and the vertical-field coils produce the compression field to achieve the compression, positioning, and equilibrium of the plasma in the radial direction.

Without considering the inside motion of the plasma, the plasma motion equations under the only influence of the external magnetic field are derived as [15]

$$\begin{cases} \dfrac{dx}{dt} = \dfrac{2\pi b^2}{\mu_0 I_p}\left[\dfrac{1}{T_s}(B_z - B_{z0} - B_{vf}) - \dfrac{dB_{vf}}{dt}\right] \\ B_z = \dfrac{\mu_0 I_p}{4\pi R}\left[\ln\dfrac{8R}{a\sqrt{k}} - \dfrac{3}{2} + \beta_p + \dfrac{l_i}{2}\right] \end{cases} \tag{14}$$

where B_z is the magnetic flux of the vertical field, B_{z0} is the programming vertical field with plasma current I_p, B_{vf} is the feedback-controlled vertical field, x is the radial displacement of the plasma, T_s is the skin-effect time constant of the coil shield to the feedback field, μ_0 is the shield permeability, b is the minor radius of the shield, R is the major radius, a is the minor radius, k is the elongation, β_p is the poloidal beta, and l_i is the internal inductance of the plasma.

Simplify the plasma motion equations and set $K_s = (2\pi b^2/\mu_0 I_p)$, so

$$B_{vf} + T_s\frac{dB_{vf}}{dt} + \frac{T_s}{K_s}\frac{dx}{dt} = B_z - B_{z0}. \tag{15}$$

Laplace transform of (17) is given as

$$x(s) = \frac{K_s}{sT_s}[B_z(s) - B_{z0}(s)] - \frac{K_s(1+sT_s)}{sT_s}B_{vf}(s). \tag{16}$$

Equation (16) is the model of the radial displacement of the plasma, which describes the relationship between the radial displacement of the plasma $x(s)$ and the feedback-controlled vertical field B_{vf}. $[B_z(s) - B_{z0}(s)]$ is the error of the vertical field to maintain the radial equilibrium of the plasma. Therefore, the control diagram of the radial magnetic compression in EAST is shown in Fig. 5, wherein the model of the plasma radial displacement is described by (16).

B. In-Vessel Vertical-Field Coils

The vertical fields for the magnetic compression of the plasma will work under pulse mode. In order to improve the compression sensitivity of the vertical field to the plasma,

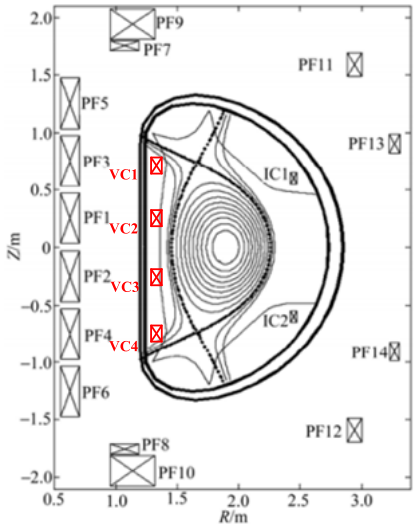

Fig. 6. Control diagram of the radial magnetic compression.

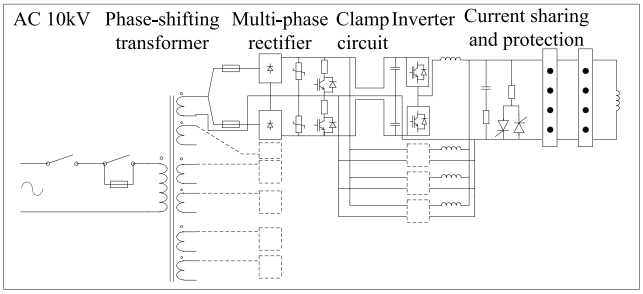

Fig. 7. Diagram of the fast-control power supply.

the required vertical-field coils should be as close to the plasma as possible, so they are designed to be placed inside the vacuum chamber.

The in-vessel vertical fields are designed to consist of four coils symmetrically located in the upper and lower parts of the vessel and connected in series. The in-vessel vertical-field coils are designed to be wound from hollow rectangle copper conductor due to its high ratio of space usage. In addition, their configuration is shown in Fig. 6.

C. Fast-Control Power Supply

The fast-control power supply for magnetic compression will be a large capacity single-phase ac/dc/ac inverter power supply, which traces the radial displacement signal of plasma and generates a vertical field for plasma radial compression, by providing thousands of amperes of excitation current to the in-vessel vertical coils.

The parameters and performance of the fast-control power supply depend on the changing rate of the radial displacement during the plasma compression. Assume that the maximal radial displacement is 0.3 m and the compression time is $<$30 ms; then the design parameters of the fast-control power supply can be derived. The output voltage is $\pm$1 k V, the maximal output current is $\pm$15 kA and the current response time is $<$5 ms.

The fast-control power supply for magnetic compression is a large capacity single-phase multilevel parallel inverter, which consists of a phase-shift transformer, rectifiers, filter and clamping circuits, inverters, and current-sharing and protection circuits, as shown in Fig. 7.

Wherein the circuit structure of the rectifier adopts the 36-pulse phase-shifting transformer combined with the noncontrolled diode rectifier. In addition, the inverter is the diode-clamped three-level inverter.

VI. Conclusion

In summary, the minor-radius compression to realize high β_p in a tokamak is described in detail in this paper.

1) The scaling range of both the major-radius and minor-radius compression is derived and plotted based on the scaling laws of the magnetic compression in a tokamak.
2) We compare the major-radius compression with the minor-radius compression. The comparison results demonstrate that the minor-radius compression has higher discharge parameters, especially for β_p, than the major-radius compression under the same additional vertical field. Then, we imagine to realize the minor-radius compression in EAST by the in-vessel vertical-field coils and take EAST shot #34128 as an example to demonstrate the scaling of the plasma shape under the in-vessel vertical field 0.04 T with $C_a = 1.5$ and $C_R = 0.925$. It is obvious for β_p to increase by 76.19%.
3) The primary scheme to realize the minor-radius compression in EAST is described. The control system of the radial magnetic compression, which includes the fast-control power supply and the in-vessel vertical-field coils, is required to control the radial displacement of the plasma during compression. The configuration, structure, and material of the in-vessel vertical fields are designed. In addition, the design parameters and the circuit diagram of the fast-control power supply are also given.

References

[1] M. Walker *et al.*, "Status of DIII-D plasma control," in *Proc. 16th IEEE/NPSS Symp. Fusion Eng., Seeking New Energy Era (SOFE)*, vol. 2. Sep. 1998, pp. 885–888.
[2] P.-A. Gourdain, J.-N. Leboeuf, and R. Y. Neches, "Stability of highly shifted equilibria in a large aspect ratio low-field tokamak," *Phys. Plasmas*, vol. 14, no. 11, p. 112513, 2007.
[3] G. Li, "The inductance of compressed plasma," *Nucl. Fusion*, vol. 55, no. 3, pp. 1–4, 2015.
[4] G. Li, "High-gain high-field fusion plasma," *Sci. Rep.*, vol. 5, pp. 1–10, Oct. 2015.
[5] H. P. Furth and S. Yoshikawa, "Adiabatic compression of tokamak discharges," *Phys. Fluids*, vol. 13, no. 10, pp. 2593–2596, 1970.
[6] E. G. Highcock *et al*, "Zero-turbulence manifold in a toroidal plasma," *Phys. Rev. Lett.*, vol. 109, no. 26, p. 265001, 2012.
[7] V. E. Golant *et al.*, "Plasma compression studies in the 'Tuman' device (CN-24/B-9)," in *Proc. 3rd Int. Conf. Plasma Phys. Controlled Nucl. Fusion Res.*, vol. 1. 1969, p. 53.
[8] K. Bol *et al.*, "Adiabatic compression of the tokamak discharge," *Phys. Rev. Lett.*, vol. 29, no. 22, pp. 1495–1498, 1972.
[9] C. C. Daughney and K. Bol, "Power balance in ATC compressed plasma," *Nucl. Fusion*, vol. 17, no. 2, pp. 367–371, 1977.
[10] K. L. Wong *et al.*, "Acceleration of beam ions during major-radius compression in the tokamak fusion test reactor," *Phys. Rev. Lett.*, vol. 55, no. 23, pp. 2587–2590, 1985.
[11] W. M. Stacey, *Fusion Plasma Physics*. New York, NY, USA: Wiley, 2012.
[12] S. Yoshikawa, "Application of the virial theorem to equilibria of toroidal plasmas," *Phys. Fluids*, vol. 7, no. 2, pp. 278–283, 1964.

[13] Q. Jinping *et al.*, "Operation with 1 MA plasma current in EAST," *Plasma Sci. Technol.*, vol. 13, no. 1, pp. 1–2, 2011.
[14] W. Baonian, L. Jiangang, G. Houyang, L. Yunfeng, and X. Guosheng, "Progress of long pulse and H-mode experiments in EAST," *Nucl. Fusion*, vol. 53, no. 10, p. 684, 2013.
[15] V. S. Mukhovatov and V. D. Shafranov, "Plasma equilibrium in a tokamak," *Nucl. Fusion*, vol. 11, no. 6, pp. 605–633, 1971.

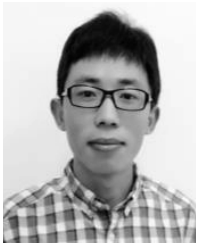

Lu Qu was born in Jiangsu, China, in 1987. He received the B.Sc. degree in automation from the Huaiyin Institute of Technology, Huai'an, China, in 2010, and the M.Eng. degree in electrical engineering from Shanghai Maritime University, Shanghai, China, in 2012. He is currently pursuing the Ph.D. degree in electrical engineering with the Institute of Plasma Physics, Chinese Academy of Sciences, Hefei, China.

He was a Power Source Designer with the Shanghai Academy of Space Technology, Shanghai. His current research interests include HVdc fault protection and pulse-power technology.

Ge Li was born in Shandong, China, in 1966. He received the B.Eng. degree in electrical engineering from the Hefei University of Technology, Hefei, China, in 1987, and the Ph.D. degree in electric machines from the Institute of Plasma Physics, Chinese Academy of Sciences (ASIPP), Hefei, in 1994.

He was a Post-Doctoral Fellow with the National Synchrotron Radiation Laboratory (NSRL), University of Science and Technology of China (USTC), Hefei, where he became an Associate Professor in 1996. After leaving Hefei in 2004, he became a Full Professor with the Department of Electrical Engineering, Shanghai Jiao Tong University, Shanghai, China, where he held this position for four years until he was back into more basic academic life for green energy investigation. He has been with NSRL, USTC, where he has been involved in accelerators and free electron lasers with Prof. D. He, the Department of Electrical and Computer Engineering, University of Manitoba, Winnipeg, MB, Canada, where he has been involved in electric machines with Prof. Menzies, and the Department of Electrical and Electronic Engineering, Newcastle University, Newcastle upon Tyne, U.K., where he has been involved in induction energy transfer with Prof. P. Acarnley. He is currently a Professor with ASIPP and the Group Leader of Transfer Cask System for ITER Remote Handing.